Received: 1 October 2017 | Revised: 22 December 2017 | Accepted: 25 January 2018

DOI: 10.1002/jbio.201700287

Journal of BIOPHOTONICS

FULL ARTICLE

Photodynamic opening of the blood-brain barrier and pathways of brain clearing

Oxana Semyachkina-Glushkovskaya[1*] | Vladimir Chehonin[2] | Ekaterina Borisova[1,3*] | Ivan Fedosov[1,4] | Anton Namykin[1,4] | Arkady Abdurashitov[1,4] | Alexander Shirokov[1,5,6] | Boris Khlebtsov[5] | Yelena Lyubun[5] | Nikita Navolokin[1,6] | Mariya Ulanova[1] | Natalia Shushunova[1] | Alexander Khorovodov[1] | Ilana Agranovich[1] | Anastasia Bodrova[1] | Madina Sagatova[1] | Ali Esmat Shareef[1] | Elena Saranceva[1] | Tatyana Iskra[1] | Mariya Dvoryatkina[1] | Ekaterina Zhinchenko[1] | Olga Sindeeva[1] | Valery Tuchin[4,7,8] | Jurgen Kurths[1,9,10]

[1]Interdisciplinary Center of Critical Technologies in Medicine, Saratov State University (National Research University), Saratov, Russia

[2]Russian National Research Medical University, Moscow, Russia

[3]Institute of Electronics, Bulgarian Academy of Sciences, Sofia, Bulgaria

[4]Research-Educational Institute of Optics and Biophotonics, Saratov State University (National Research University), Saratov, Russia

[5]Institute of Biochemistry and Physiology of Plants and Microorganisms, Russian Academy of Sciences (IBPPM RAS), Saratov, Russia

[6]Saratov State Medical University, Saratov, Russia

[7]Tomsk State University (National Research University), Tomsk, Russia

[8]Institute of Precision Mechanics and Control, Russian Academy of Sciences (IPMC RAS), Saratov, Russia

[9]Physics Department, Humboldt University, Berlin, Germany

[10]Potsdam Institute for Climate Impact Research, Potsdam, Germany

***Correspondence**
Oxana Semyachkina-Glushkovskaya, Interdisciplinary Center of Critical Technologies in Medicine, Saratov State University (National Research University), 83 Astrakhanskaya street, 410012 Saratov, Russia.
Email: glushkovskaya@mail.ru
Ekaterina Borisova, Institute of Electronics, Bulgarian Academy of Sciences, Tsarigradsko Chaussee 72, Sofia 1784, Bulgaria.
Email: borisova@ie.bas.bg

Funding information
Russian Science Foundation, Grant/Award number: 17-15-01263

A new application of the photodynamic treatment (PDT) is presented for the opening of blood-brain barrier (BBB) and the brain clearing activation that is associated with it, including the use of gold nanoparticles as emerging photosensitizer carriers in PDT. The obtained results clearly demonstrate 2 pathways for the brain clearing: (1) using PDT-opening of BBB and intravenous injection of FITC-dextran we showed a clearance of this tracer via the meningeal lymphatic system in the subdural space; (2) using optical coherence tomography and intraparenchymal injection of gold nanorods, we observed their clearance through the exit gate of cerebral spinal fluid from the brain into the deep cervical lymph node, where the gold nanorods were accumulated. These data contribute to a better understanding of the cerebrovascular effects of PDT and shed light on mechanisms, underlying brain clearing after PDT-related opening of BBB, including clearance from nanoparticles as drug carriers.

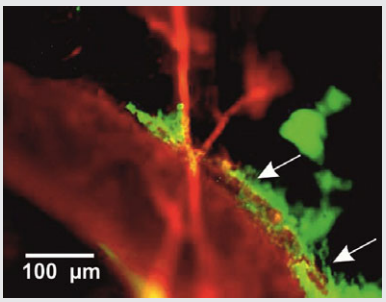

KEYWORDS

blood-brain barrier, cerebral lymphatic vessels, gold nanorods, optical coherence tomography, photodynamic treatment

1 | INTRODUCTION

The blood-brain barrier (BBB) is a highly selective "custom" coupled with multiple specific transport systems on microvascular endothelial cells that prevents passage of most biological molecules and circulating cells. The crucial physiological role of BBB is to protect the central nervous system (CNS) against pathogens and toxic substances. However, this protective mechanism limits 98% of the beneficial drugs delivery to the CNS [1, 2]. This is the reason, why diseases of the brain and spinal cord continue to cause some of the most dramatic disability in society. Stroke, epilepsy and mental illness (neurosis and depression) have a very high morbidity and mortality rates [3]. Therefore, the absence of effective methods for brain drug delivery is a key hurdle in the progress of neuroscience and neuropharmacology; this explains significant researcher's attention to the development of breakthrough technologies for the opening of BBB [4–6]. However, none of the nearly 70 methods developed so far in this field is being widely applied to the everyday clinical practice, due to the many limitations they possess, including invasiveness, challenges in performing or provision of a sufficient therapeutic drug dose and small area of treatment [7–9].

The photodynamic treatment (PDT) is a widely used clinical method for fluorescence-guided resection of malignant gliomas. The recent studies of Hirschberg et al. and Madsen et al. on rats have been shown that PDT effectively opens the BBB [10–13]. In our experiments on mice, we demonstrated the application of PDT for the temporary increase of the BBB permeability to high-molecular weight molecules [14]. We found that the optimal laser dose for the BBB opening at 635 nm was 15 J/cm^2 for a concentration of 5-aminolevulinic acid (5-ALA) of 20 mg/kg, iv.

For surgical navigation, some authors have recommended the use of a laser emitting at 635 nm and a dose of protoporphyrin IX precursor 5-ALA of 20 mg/kg [15–17]. These PDT parameters are similar to those used by us for the BBB opening [14]. It is well known that an adverse effect of PDT-rejection of a brain tumor is a perivascular edema, or accumulation of an extensive amount of water in the area around the cerebral vessels, which induces an increase in the intracerebral pressure [18]. The effects of PDT on the BBB function might be among the reasons for changes in the balance of water in the brain.

The lymphatic system plays a pivotal role in the drainage of water in peripheral circulation. However, despite the recent discovery of the meningeal lymphatic vessels [19, 20], their role in clearing the brain is still questionable and needs further detailed studies.

To achieve a better understanding of PDT's cerebrovascular effects, we explored the clearing and recovery of the brain after PDT-opening of the BBB by focusing our attention on the lymphatic pathway and making use of specific lymphatic vessels markers, confocal imaging and histological analysis. Furthermore, bearing in mind the extensive use of nanoparticles as photoactivated compounds and their emerging application as photosensitizer drug carriers, we studied the brain clearing from gold nanorods injected into the brain parenchyma [21, 22].

2 | MATERIALS AND METHODS

2.1 | Subjects

Male mice (20-25 g) were used in all experiments. The animals were housed under standard laboratory conditions, with access to food and water, ad libitum. All procedures were performed in accordance with the "Guide for the Care and Use of Laboratory Animals". The experimental protocol was approved by the Committee for the Care and Use of Laboratory Animals at Saratov State University (Protocol H-147, April 17, 2001). The studies involved 2 groups: (1) a control group, including animals without PDT ($n = 10$); (2) the experimental group included mice exposed to PDT ($n = 17$).

2.2 | PDT protocol

The mice were anesthetized by ketamine (100 mg/kg) and xylazine (10 mg/kg, i.p.), and fixed in a stereotactic frame. The PDT was performed 30 minutes after intravenous injection of 5-ALA (20 mg/kg). The epicranium was exposed by a parieto-occipital midline skin incision. With the use of a microsurgical technique, the periosteum was pushed back and biparietal parasagittal groove-shaped trephinations (2×2 mm) was performed with a microdrill (Mikroton, Aesculap, Pennsylvania, USA) accompanied by continuous irrigation with saline to prevent heating of the tissue. Special care was taken to avoid penetration of the dura mater.

For irradiation, we used a high-power continuous-wave red LED (XPeBRD-L1-0000-00901, CREE, Inc., Durham, North Carolina, USA) emitting up to 1 W output light power at 635 nm, with a possibility to control the emitted-light power-density in the range 20 to 200 mW/cm^2 at a step of 10 mW/cm^2, as measured on the tip of an 8-mm-diameter solid light-guide. The spectral width of the emitted-light at full width at half maximum (FWHM) of intensity was 30 nm. The mouse brains were irradiated at a constant power-density of 40 mW/cm^2 and an exposure time of 375 seconds, thus achieving a light dose of 15 J/cm^2. The brain tissue heating due to the laser light was followed by a Pico USB TC-08 thermocouple data logger (Cambridgeshire, UK). The temperature rise did not exceed 2°C above the mouse body level of 28°C for the irradiation dose chosen.

2.3 | Assessment of BBB permeability

To analysis the BBB permeability to high-molecular weight substances, we used a confocal imaging of FITC-dextran

70 kDa extravasation [23]. In brief, 1.5 hours after PDT when the BBB was opened [14], FITC-dextran was injected intravenously (4 mg/25 g mouse, 0.5% solution in 0.9% physiological saline, Sigma) and circulated 2 minutes. The mice then were decapitated and brains were quickly removed and fixed in 4% paraformaldehyde for 24 hours, cut into 50-μm thick slices on vibratome (Leica VT 1000S Microsystem, Wetzlar, Germany) and analyzed by a confocal microscope TCS SP5 (Leica-microsystems). Approximately 8 to 12 slices per animal from cortical and subcortical (excepting hypothalamus and choroid plexus where the BBB is leaky) regions were obtained and imaged.

The BBB permeability to low molecular weight molecules (solutes) was analyzed histologically. All mice were decapitated, and the samples were fixed in 10% buffered neutral formalin. The formalin fixed specimens were embedded in paraffin, sectioned (4 μm) and stained with hematoxylin and eosin. The histological sections were evaluated by light microscopy using a Mikrovizor μVizo-103 digital image medical analysis system (LOMO, St. Petersburg, Russia).

2.4 | Study of the brain clearing after PDT-related opening of BBB ex vivo and in vivo

To study the brain clearing via the meningeal lymphatic system after PDT, we used FITC-dextran 70 kDa, which extravasated from the cerebral vessels into the brain parenchyma through the PDT-opened BBB and was estimated by confocal and fluorescent microscopy.

Briefly, the experimental procedure was as follows: 1.5 hours after PDT (see protocol for PHD) when the BBB was opened [14], FITC-dextran 70 kDa was injected intravenously (1 mg/25 g mouse, 0.5% solution in 0.9% physiological saline, Sigma-Aldrich, St. Louis, USA) and allowed to circulate for 2 minutes. To label the lymphatic vessels, after FITC-dextran infusion, mice were injected i.c.v. (into the cisterna magna) with 5 mL of Alexa 488-conjugated anti-LYVE-1 antibody (ALY7, eBioscience, San Diego, USA) as described in Ref. [19].

In the in vivo experiments, 10 minutes after this procedure, the brain clearing from FITC-dextran in anesthetized mice was evaluated using a fluorescent microscope (Carl Zeiss Microscopy GmbH, Jena, Germany), equipped with a CMOS camera (acA1920-40uc, Basler AG, An der Strusbek, Ahrensburg, Germany) and a 10 × 0.3 objective lens. To visualize the Alexa-488 and FITC-dextran, mounted filter sets 49 002, 49 004 (Chroma Technology Corp., Vermont, USA) were used, respectively.

Following the ex vivo experiments, the mice were decapitated; their brains were quickly removed, fixed in 4% PFA for 24 hours, cut into 50-μm thick slices on a vibratome (Leica VT 1000S Microsystem) and analyzed by a confocal microscope (Olympus FV10i-W, Olympus, Japan). Approximately 10 slices per animal were imaged.

2.5 | Nanorods preparation and injection into the brain

2.5.1 | Procedures of preparation and characterization of gold nanorods

Gold nanorods (GNRs), coated with thiolated polyethylene glycol, were prepared by seed mediated growth in binary surfactant mixture as described elsewhere [24, 25]. Extinction spectra were measured by a Specord 250 spectrophotometer (Analytik, Jena, Germany). Transmission electron microscopy (TEM) images were recorded on a Libra-120 transmission electron microscope (Carl Zeiss, Jena, Germany) at the Symbiosis Center of Collective Usage of Research Equipment in the Field of Physical-Chemical Biology and Nanobiotechnology of IBPPM RAS, Saratov (CCU IBPPM RAS). Analyzing the TEM images of the GNR suspensions, we estimated the average nanoparticle diameter and length at 16 ± 3 nm and 92 ± 17 nm, respectively.

The GNRs content in the brain tissues was evaluated by atomic absorption spectroscopy on a Dual Atomizer Zeeman AA iCE 3500 spectrophotometer (Thermo Scientific Inc., Waltham, Massachusetts, USA) in the CCU IBPPM RAS, calibrated using the standard for AAC (Fluke, Everett, WA, USA). The process of tissue sample preparation was carried out in an automatic mode with a constant control of the temperature in a MARS Xpress (Matthews, NC, USA) microwave system. For all measurements performed, the SD did not exceed 4%.

2.5.2 | Intraparenchymal injection of GNRs

The mice were anesthetized by ketamine (100 mg/kg, i.p.) and xylazine (10 mg/kg, i.p.), and fixed in a stereotactic frame. A midline skin incision was made to reveal the skull bone, which was thinned with a dental drill to 2 mm lateral and 2.5 mm caudal to the bregma. GNRs (7 μL) was injected into a 2-mm depth from the bregma in 0.5 μL with a 34-G Hamilton needle at a 0.1 μL/min rate over 5 minutes with a syringe pump (Harvard Apparatus, Holliston, USA). These experiments were performed on 10 healthy mice.

2.6 | Optical coherence tomography measurements

Optical coherence tomography (OCT) is a tool allowing one to obtain high resolution, depth-resolved images of inhomogeneities within scattering media; it makes use of dual-beam interference created by a broad-band light source to select ballistic photons (ie, specular photons reflected back off each interface between 2 adjacent tissue layers with different refractive indices) [26]. Since lymph is optically transparent within a broad range of wavelengths, “empty” cavities exist in the resulting OCT image of the lymphatic node with a background signal-to-noise ratio inside (see Figure 3C-D). In order to visualize the dynamic accumulation of lymph within these cavities, suspensions of GNRs were used as contrast agents, the OCT signal intensity being proportional to the GNRs concentration. By tracking the OCT signal temporal intensity changes inside a node’s cavity, we could confirm the clearing pathways and calculate its relative speed. The

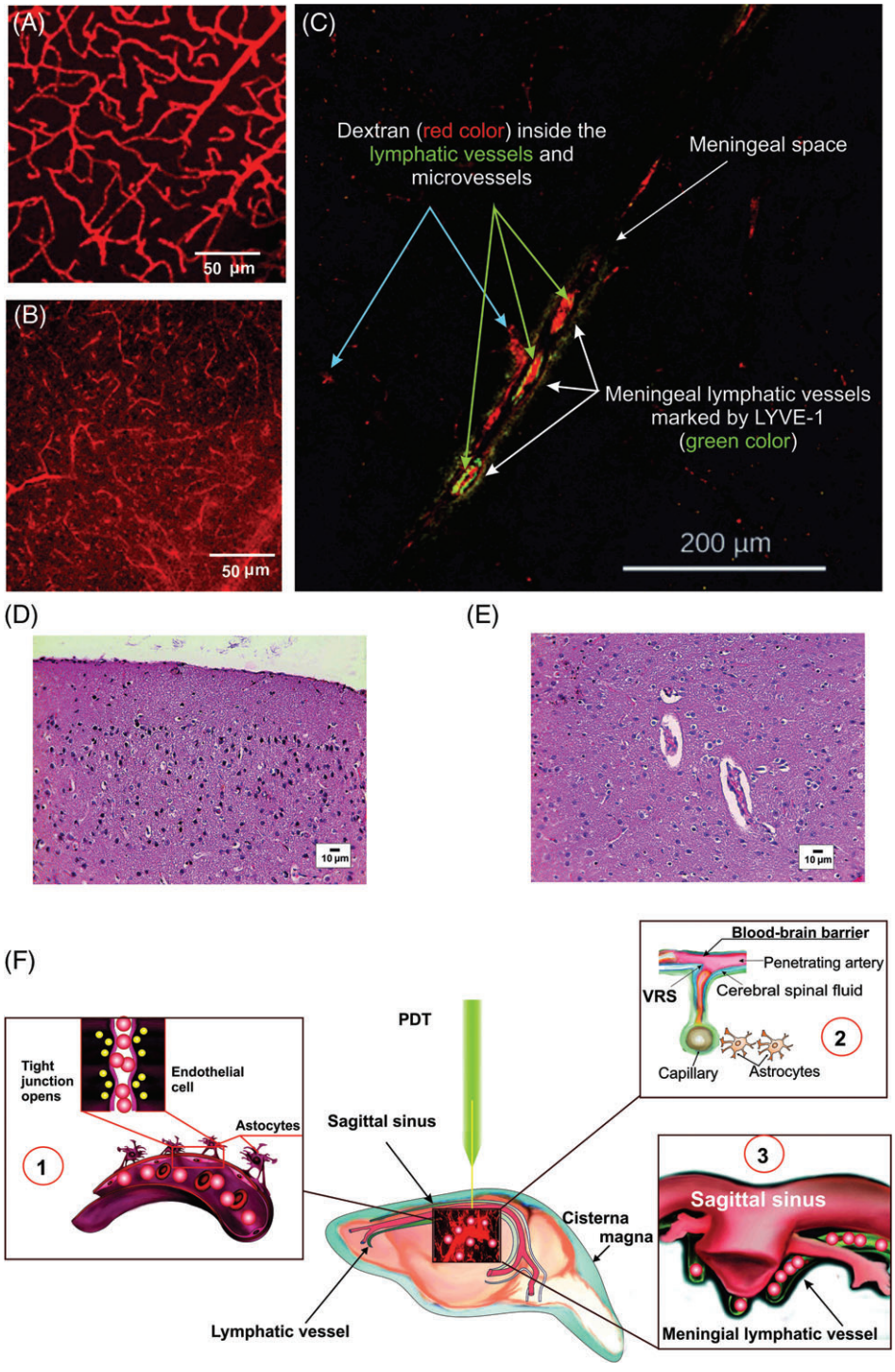

FIGURE 1 Photodynamic opening of the blood-brain barrier. (A) No extravasation of FITC-dextran 70 kDa before PDT; (B) Strong extravasation of FITC-dextran 70 kDa 1.5 h after PDT (defined as many red clouds around a group of microvessels); (C) Confocal imaging of the meningeal lymphatic vessels marked by specific antibodies (LYVE-1—green color) with presence of FITC-dextran in them (red color) 30 minutes after the PDT-opening of BBB. (D, E) Histological analysis of cerebral vessels before (D) and after (E) PDT-opening of BBB: PDT-opening of BBB was associated with the development of moderate perivascular edema observed 1.5 hour after the PDT. Hematoxylin and Eosin staining. Bars represent 10 μm (246.4×). (F) Schematic illustration of possible pathways underlying the brain clearing from FITC-dextran after PDT-opening of BBB: (1) PDT-opening of BBB; (2) movement of FITC-dextran from the brain parenchyma into the VRS; (3) movement of FITC-dextran from the VRS into the meningeal lymphatic vessels (hypothesis is based on literature review [27–29])

OCT recordings were performed under anesthesia with ketamine (100 mg/kg, ip) and xylazine (10 mg/kg, ip).

2.7 | Statistical analysis

The results were reported as a mean value ± standard error (SE) of the mean (SEM). Differences from the initial level in the same group were evaluated by the Wilcoxon test. Intergroup differences were evaluated using the Mann-Whitney test and ANOVA-2 (post hoc analysis with the Duncan's rank test). The significance levels were set at $P < .05$ for all analyses.

3 | RESULTS AND DISCUSSION

3.1 | Photodynamic opening of BBB and brain clearing via the meningeal lymphatic system

In these series of experiments, we studied a PDT-opening of the BBB and the associated with it the brain clearing activation via the meningeal lymphatic system.

Figure 1A,B shows confocal imaging of cerebral vessels before and after PDT illustrating the high permeability of BBB to FITC-dextran 70 kDa. The dextran extravasation was determined based on the specific fluorescence occurring outside of

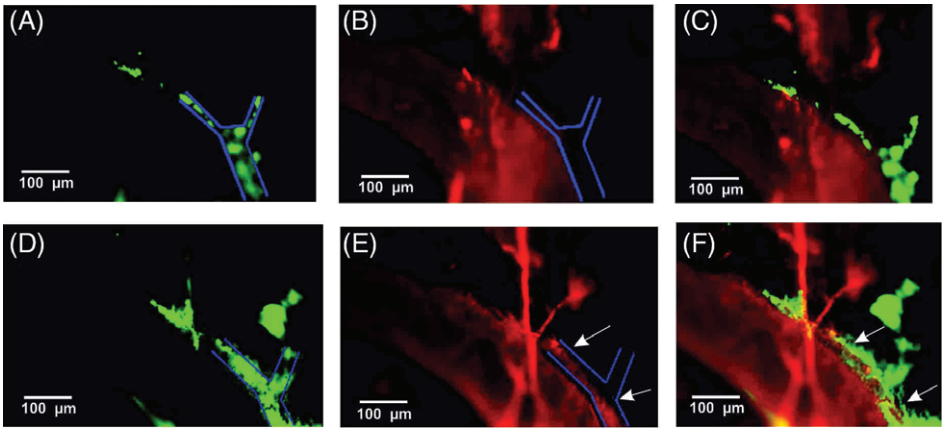

FIGURE 2 Fluorescent microscopy of the brain clearing from the FITC-dextran via the meningeal lymphatic vessels after PDT-opening of BBB. Before PDT-opening of the BBB: (A) meningeal lymphatic vessels marked by specific antibodies (LYVE-1—green color, blue lines delineate the boundaries of the lymphatic vessel); (B) FITC-dextran presence inside the Sagittal sinus (the main cerebral vein), but not in the meningeal lymphatic vessel after its intravenous injection; (C) merged pictures of A and B. After PDT-opening of the BBB: (D) the same as in (A); (E) FITC-dextran presence inside the Sagittal sinus and in the meningeal lymphatic vessel (arrowed) after its extravasation from the cerebral vessels into the brain parenchyma; (F) merged pictures of (D) and (E)

the vessel walls and was classified as weak (+), medium (++), strong (+++) and diffusive (++++) [23]. A faint cloud, clearly associated with one vessel site of tracer leakage, was defined as a weak infiltration. A medium infiltration referred to a bright cloud, clearly associated with one vessel site of tracer leakage. A strong one meant a bright cloud, not clearly associated with one vessel leakage, but with a group of vessels. Diffusive infiltration consisted in an extensive leakage of tracer, without a clear association with specific vessels.

Our results showed that the light exposure of 15 J/cm^2 with 5-ALA tissue sensitization (20 mg/kg, i.v.) was associated 1.5 hours afterwards with strong leakage of FITC-dextran from cerebral capillaries, resulting in formation of many red fluorescent clouds around microvessels (Figure 1B).

As an additional method for studying the BBB opening, we conducted a histological examination of the entire brain's vascular permeability to solutes. A moderate perivascular edema around enlarged capillaries due to excessive blood presence was observed 30 minutes after PDT-opening of the BBB, suggesting a high BBB permeability to solutes (Figure 1E). Three days later, the cerebral vessels and tissues histological picture was similar to that of the control group, that is, the BBB permeability to solutes had recovered completely (Figure 1D).

In the next step of our work, we studied how the brain cleans itself from FITC-dextran after PDT-opening of the BBB focusing on the meningeal lymphatics, which was marked by specific antibodies—lymphatic vessel endothelial receptor 1 (LYVE-1), responsible for the transport of different molecules via the lymphatic vessels endothelium). Figure 1C presents confocal imaging of the meningeal lymphatic vessels 30 minutes after PDT-opening of the BBB. The choice of this time period was prompted by the results of Louveau et al. who reported brain clearing from the Evans Blue tracer 30 minutes after injection into the brain parenchyma [19].

Our ex vivo confocal results clearly showed the presence of FITC-dextran inside of the meningeal lymphatic vessels after its passage into the brain tissues through the opened BBB (Figure 1C).

The in vivo fluorescent microscopy confirmed the ex vivo confocal data. Indeed, the presence of FITC-dextran inside the meningeal lymphatic vessels 30 minutes after a PDT-opening of the BBB is clearly visible in Figure 2E,F, suggesting brain clearing from FITC-dextran, which has passed through the BBB and extravasated from the cerebral vessels into the brain parenchyma. The brain clearing was associated with enlarged lymphatic vessels. Thus, the average diameter of the meningeal lymphatic vessels was a 2.3-fold larger (23 $\pm$ 0.03 μm vs 10 $\pm$ 0.01 μm) after PDT-opening of BBB compared to the control group (before the PDT) reflecting the activation of brain drainage via the meningeal lymphatic system. These data are in agreement with our previous results obtained using a sound-opening of BBB [30].

In the 18th century Italian anatomist Paolo Mascagni and recently, in 2015 Louveau et al. and Aspelund et al. described the architecture of the meningeal lymphatic vessels, which localize superficially in the subdural area along the cerebral sinuses [19, 20, 31].

These facts together suggest a functional and anatomical connection between the brain parenchyma, where is anatomical location of BBB in microvessels and the superficial meningeal lymphatic vessels. Probably the Virchow-Robin space (perivascular space) is the connective bridge between the BBB and the meningeal lymphatic system; this hypothesis has been actively discussed during past 2 decades [27–29] as a hypothesis. Figure 1F is a schematic illustration of this suggestion.

3.2 | Brain clearing from gold nanorods: optical coherence tomography study

As photoactivated compounds, nanoparticles have in recent years emerged as promising photosensitizer carriers in PDT

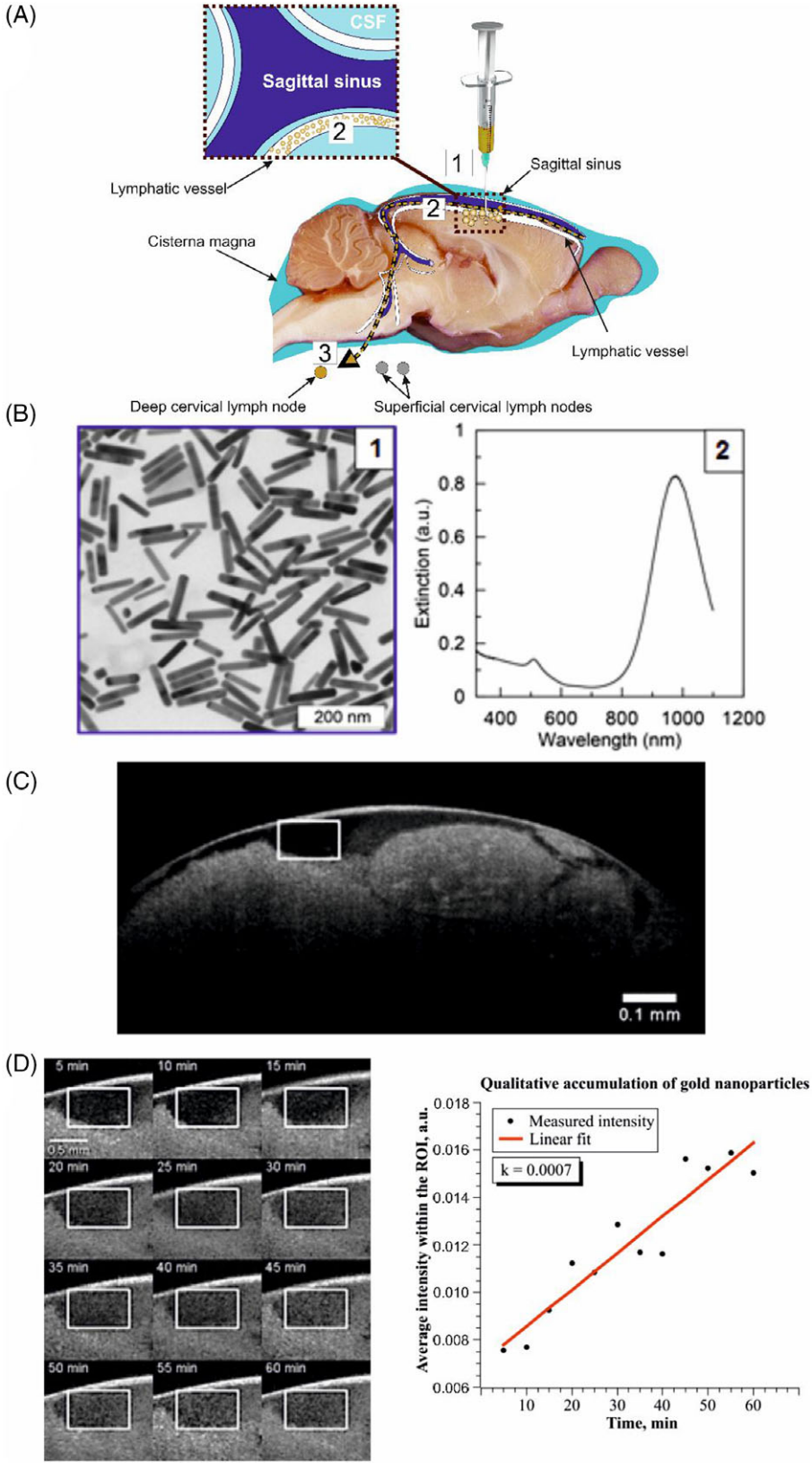

FIGURE 3 OCT imaging of brain clearing from GNRs: (A) experimental scheme illustration: (1) GNRs are injected into the brain parenchyma; (2) GNRs drain from the brain via the meningeal lymphatic vessels; (3) 20 minutes after injection, GNRs are accumulated in the deep cervical lymph node; (B) transmission electron microscopy image of GNRs (92 × 16 nm) (1) and their extinction spectrum (2); (C) OCT image of the deep cervical lymph node before injection of GNRs; (D) a set of OCT images illustrating the kinetics of accumulation of GNRs in the deep cervical lymph node after intraparenchymal injection of GNRs; (E) OCT signal's average intensity within the region of interest showing linear accumulation of GNRs in the deep cervical node with slope $k = 0.0007$. Detailed k value interpretation is given in the text. OCT images were acquired using commercial Thorlabs system GANYMEDE (Thorlabs Inc., Newton, New Jersey, USA). 30KHz A-scan rate, 930 nm – central wavelength, 150 nm – spectrum bandwidth, axial resolution 5.8/4.4 μm in air/water, respectively

[21, 22]. However, how the brain clean itself of nanomaterials is yet to be understood. In attempt to contribute to clarifying this phenomenon, we studied the brain clearing from GNRs injected into the brain parenchyma; using OCT, we analyzed the accumulation of GNRs in the deep cervical lymph node as the first anatomical station for the exit of cerebral spinal fluid (CSF) from the brain [32, 33].

Figure 3 A is a schematic illustration of the experiment. Figure 3B-1 presents transmission electron microscopy images of GNRs (92 × 16 nm) with an axial ratio of 5.7. This corresponds well with the positions of the longitudinal

(975 nm) and transverse (507 nm) resonances seen in the extinction spectrum (Figure 3B-2).

Figure 3D shows that the injection of GNRs into the brain parenchyma produced a strong rise in the back-scattered signal 20 minutes after the injection. This fact allowed us to image the kinetics of GNRs accumulation in the deep cervical lymph node. A preinjected B-mode image of the lymphatic node is shown on Figure 3C; the white rectangle delineates the region of interest, where intensity changes were observed due to the accumulation of highly-scattering GNRs. Figure 3D is a time-lapse set of OCT images as GNRs accumulate within the node's cavity. Figure 3E presents the approximately linear time dependence of the spatially averaged OCT signal intensity within the region of interest. Differentiating the approximation function (red line) we obtained its slope, namely $k = 0.0007$, which is indicative of the rate (in arbitrary volumetric units) at which the CSF flows from the point of injection to the deep cervical node. The rise in the OCT signal intensity is caused by the increased number of GNRs within the node's cavity. Therefore, another interpretation of the k constant is the rate of change in GNRs concentration. To obtain qualitative information about the volumetric CSF flow rate, a careful calibration process is required to relate the concentration of nanoparticles to the OCT signal intensity changes.

Atomic absorption spectroscopy showed that after the injection of GNRs, the concentration of gold in the brain parenchyma was 1.04 ± 0.07 μg/g of tissue; 20 minutes after injection, the level of gold decreased by a 1.7-fold (0.61 ± 0.03 μg/g, $P < 0.05$) in the brain with gold significant accumulation in the deep cervical lymph node (14.5 ± 3.7 μg/g, $P < .05$).

Collectively, our results showed that PDT causes an opening of the BBB, in agreement with our previous data and Hirschberg's results [10, 14]. We clearly revealed a PDT-related increase in the BBB permeability to FITC-dextran 70 kDa. Using histological analysis of the brain tissues, we also demonstrated a PDT-related opening of the BBB to solutes.

The processes after PDT-opening of the BBB were accompanied by brain clearing via the meningeal lymphatic vessels. Indeed, 30 minutes after the PDT-related opening of the BBB for FITC-dextran, our ex vivo (confocal data) and in vivo (fluorescent microscopy) experiments pointed to the presence of this tracer inside the meningeal lymphatic vessels, which were marked by specific antibodies (LYVE-1). These results are consistent with our earlier results, obtained using a sound-induced model of BBB opening, indicating brain clearing from FITC-dextran via the meningeal lymphatic vessels [30].

The nanoparticles are promising compounds for PDT as emerging photosensitizer carriers [21, 22]. Therefore, the next step of our work was focused on the study of brain clearing from GNRs. Our results definitely showed that 20 minutes after injection of GNRs into the brain parenchyma, the GNRs were accumulated in the deep cervical lymph node. Similar results have been shown by others, who demonstrated the transfer of different tracers from the brain parenchyma directly into the deep cervical lymph node [32, 33]. Louveau et al. and Aspelund et al. experimentally demonstrated the pivotal role of the meningeal lymphatic system in the brain clearing. Other researchers actively discussed the mechanisms underlying movement of CSF independently on the lymphatic system in the brain [19, 20]. However, currently no explanation exists, how the molecules move from the brain parenchyma to the superficial lymphatic vessels, or into the CSF. The Virchow-Robin space or perivascular space is one of possible pathway in these hypotheses, however, it is a virtual space because it is difficult to be detected in normal conditions and only a cerebral pathology is associated with the appearance of this Virchow-Robin space (VRS) [30]. Our data support both these hypotheses, because we observed an appearance of the tracer (FITC-dextran) in the meningeal lymphatic vessels after its crossing of the BBB and an accumulation of GNRs in the deep cervical lymph node (the first anatomical station for the exit of CSF from the brain) after their injection in the brain parenchyma.

4 | CONCLUSION

With a high degree of certainty, our results point to the PDT, inducing a BBB opening and, further, activation of a brain clearing process, which can also be observed after injection of GNRs into the brain parenchyma. Two pathways are possible for brain clearing: (1) via the meningeal lymphatic system through the subdural space in the case of PDT-opening of the BBB; (2) via the gate of exit of CSF from the brain in the case of clearance of GNRs injected into the brain parenchyma. We believe that these 2 pathways are closely connected; proving this proposition, however, would require additional detailed studies and will be discussed in further publications. Moreover, these data shed light on a new PDT application as a technique of brain drug delivery and the brain clearing activation related with it.

ACKNOWLEDGMENT

This work supported by Grant of Russian Science Foundation No 17-15-01263.

AUTHOR BIOGRAPHIES

Please see Supporting Information online.

REFERENCES

[1] W. M. Pardridge, *Drug Discov. Today* **2007**, *12*, 54.
[2] A. K. Ghose, V. N. Viswanadhan, J. J. Wendoloski, *J. Comb. Chem.* **1999**, *1*, 55.

[3] A. Pan, Q. Sun, O. I. Okereke, K. M. Rexrode, F. B. Hu, *JAMA* **2011**, *306*(11), 1241.
[4] M. Hammarlund-Udenaes, E. de Lange, R. Thorne (Eds,), Springer, Berlin **2014**.
[5] S. Mitragotri, *Adv. Drug Deliv. Rev.* **2013**, *65*, 100.
[6] P. K. Pandey, A. K. Sharma, U. Gupta, *Tissue Barriers* **2016**, *4*, e1129476.
[7] V. Kiviniemi, *PLoS ONE* **2017**, *12*, e0174072.
[8] S. Wu, *J. Clin. Cell. Immunol.* **2013**, *4*, 24244890.
[9] P. C. Chu, *Sci. Rep.* **2016**, *6*, 33264.
[10] H. Hirschberg, *Lasers Surg. Med.* **2008**, *40*, 535.
[11] S. J. Madsen, *J. Biophotonics* **2010**, *3*, 356.
[12] S. J. Madsen, *Lasers Surg. Med.* **2013**, *45*, 524.
[13] S. J. Madsen, *Lasers Med. Sci.* **2015**, *4*, 1357.
[14] O. Semyachkina-Glushkovskaya, *BOE* **2017**, *8*(11), 5040.
[15] W. Stummer, *Neurosurgery* **2017**, *81*, 230.
[16] M. J. Colditz, *J. Clin. Neurosci.* **2012**, *19*, 1471.
[17] T. Kuroiwa, *Prog. Neuro Oncol.* **2014**, *21*, 14.
[18] M. Mathews, D. Chighvinadze, H. Michael Gach, F. Uzal, S. Madsen, H. Hirschberg, *Lasers Surg. Med.* **2011**, *43*(9), 892.
[19] A. Louveau, I. Smirnov, T. Keyes, J. Eccles, S. Rouhani, J. Peske, N. Derecki, D. Castle, J. Mandell, K. Lee, T. Harris, J. Kipnis, *Nature* **2015**, *523*, 337.
[20] A. Aspelund, S. Antila, S. Proulx, T. Karlsen, S. Karaman, M. Detmar, H. Wiig, K. Alitalo, *J. Exp. Med.* **2015**, *212*(7), 991.
[21] D. Bechet, C. Frochot, R. Vanderesse, M. Barberi-Heyob, *J. Carcinog. Mutagen.* **2012**, *S8*, 001. https://doi.org/10.4172/2157-2518.S8-001.
[22] H. Yuan, C. M. Wilson, J. Xia, S. L. Doyle, S. Li, A. M. Fales, Y. Liu, E. Ozaki, K. Mulfaul, G. Hanna, G. M. Palmer, L. V. Wang, G. A. Grant, T. Vo-Dinh, *Nanoscale* **2014**, *6*(8), 4078.
[23] A. Hoffmann, *Transl. Stroke Res.* **2011**, *2*, 106.
[24] B. Khlebtsov, V. Khanadeev, G. Sukhorukov, N. Khlebtsov, *Langmuir* **2014**, *30*, 1696.
[25] Y. Zheng, J. Chen, C. Murray, *Nano Lett.* **2013**, *13*, 765.
[26] A. Fercher, W. Drexler, C. Hitzenberger, T. Lasser, *Rep. Prog. Phys.* **2003**, *66*(2), 239.
[27] S. Hladky, M. Barrand, *Fluids Barriers CNS* **2014**, *11*, 26.
[28] M. Johnston, C. Papaiconomou, *News Physiol. Sci.* **2002**, *17*, 227.
[29] L. Koh, A. Zakharov, M. Johnston, *Cerebrspinal Fluid Res.* **2005**, *2*, 1.
[30] O. Semyachkina-Glushkovskaya et al., *J. Biomed. Opt.* **2017**, *22*(12), 121719.
[31] P. Mascagni, G.B. Bellini, Istoria Completa Dei Vasi Linfatici, Vol. II. Presso Eusebio Pacini e Figlio, Florence **1816**, 195 pp.
[32] M. Bradbury, H. Cserr, R. Westrop, *Am. J. Physiol.* **1981**, *240*, 329.
[33] H. Cserr, C. Harling-Berg, P. Knopf, *Brain Pathol.* **1992**, *2*, 269.

How to cite this article: Semyachkina-Glushkovskaya O, Chehonin V, Borisova E, et al. Photodynamic opening of the blood-brain barrier and pathways of brain clearing. *J. Biophotonics*. 2018;11: e201700287. https://doi.org/10.1002/jbio.201700287